1 Introduction and Concepts

Abstract

This chapter presents a brief introduction to marine carbonate chemistry systematics, including definitions of different pH scales. As a starting point, published estimates of Pleistocene and Cenozoic pCO_2 reconstructions from boron isotopes and B/Ca ratios in planktic foraminifera are shown in the context of ice core records and reconstructions from terrestrial leaf stomata and marine alkenones. These published boron proxy records form the foundation for discussing boron proxy systematics and sensitivity studies presented in the following chapters.

Keywords: atmospheric pCO_2; seawater carbonate chemistry; seawater pH; pH scales

1.1 Why Are we Interested in Reconstructing Marine Carbonate Chemistry?

It has been known since the early studies of Arrhenius (1896) that anthropogenic emissions of carbon dioxide from fossil fuel burning and land use changes will warm our planet, but direct evidence for increasing atmospheric pCO_2 levels emerged only in 1958, when Charles Keeling started continuous measurements at the Mauna Loa Observatory on Hawaii and initially observed an average annual value of 315 parts per million (ppm) (Keeling et al. 1976). These atmospheric pCO_2 levels varied seasonally, steadily increased year upon year and were finally put into perspective when Raynaud and Barnola (1985) presented the first pCO_2 measurements from Antarctic ice cores, which revealed pre-anthropogenic background levels as

Boron Proxies in Paleoceanography and Paleoclimatology, First Edition. Bärbel Hönisch, Stephen M. Eggins, Laura L. Haynes, Katherine A. Allen, Katherine D. Holland, and Katja Lorbacher.

Companion website: www.wiley.com/go/Hönisch/Boron_Paleoceanography

low as 260 ppmv (parts per million by volume). Subsequent studies expanded the ice core records to 800 000 years ago and constrained the pre-industrial range of atmospheric pCO_2 to 172–300 ppmv, together with concomitant Antarctic temperature fluctuations of ~12 °C (Barnola et al. 1987; Jouzel et al. 1987; Lüthi et al. 2008; Petit et al. 1999; Siegenthaler et al. 2005). In 2014 atmospheric pCO_2 hit 400 ppm for the first time (Dlugokencky and Tans 2017) and levels are projected to climb to 420–940 ppm by the end of this century, depending on future emissions (Figure 1.1).

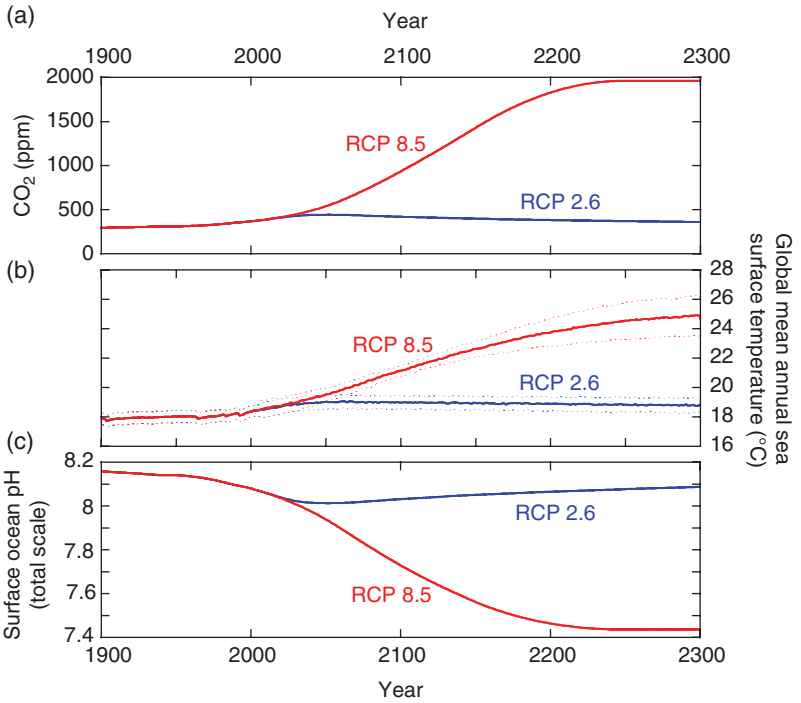

Figure 1.1 Historical observations and future trends in (a) atmospheric pCO_2 (Meinshausen et al. 2011), (b) global sea surface temperature, and (c) surface ocean pH as a function of two CO_2 emission scenarios – Representative Concentration Pathways RCP2.6 and RCP8.5. These scenarios represent the full range of possible future CO_2 emissions used by scientists to predict future climate trends (see also IPCC 2013). Future sea surface temperature trends are globally averaged multi-model estimates extracted from CMIP5 numerical experiments (Moss et al. 2010; Taylor et al. 2011), where temperature uncertainties are based on differences between individual model outputs. pH has been calculated in CO2SYS (Pierrot et al. 2006), with K_1 and K_2 according to Lueker et al. (2000), K_{SO4} according to Dickson (1990), total [B] after Lee et al. (2010). Calculations have been parameterized using pCO_2 and T as displayed in (a) and (b), S = 35, and adopting total alkalinity AT = 2300 µmol kg^{-1} as the second parameter required for seawater carbonate chemistry calculations. The temperature uncertainties displayed in (b) exert negligible influence on the pH estimates and do not exceed the thickness of the lines displayed in (c). Depending on the actual extent of future emissions, ocean acidification may peak at pH ~ 8.0 (TS, RCP2.6) or fall to pH < 7.3 (TS, RCP8.5). Predicting ocean ecosystem responses to such acidification remains a challenge but may be improved by studying carbonate chemistry perturbations in Earth's geological past.

While discussion of the consequences of rising atmospheric pCO_2 initially concentrated on global warming, research over the past two decades has increasingly addressed the dissolution of CO_2 in seawater and its consequences for marine life. Briefly, as CO_2 dissolves in the ocean, it hydrates and reacts with water to form carbonic acid, which then dissociates into bicarbonate, carbonate, and hydrogen ions according to the following reactions:

$$CO_2 + H_2O \longleftrightarrow H_2CO_3 \longleftrightarrow HCO_3^- + H^+ \longleftrightarrow CO_3^{2-} + 2H^+ \quad (1.1)$$

The more CO_2 dissolves, the more hydrogen ions are created but these ions do not immediately accumulate, as they are buffered by the carbonate ions already in solution:

$$CO_3^{2-} + H^+ \longleftrightarrow HCO_3^- \quad (1.2)$$

However, a small fraction of the resulting bicarbonate ions will dissociate, ultimately increasing the hydrogen ion concentration and therefore the acidity of seawater (i.e. lowering pH):

$$HCO_3^- \longleftrightarrow CO_3^{2-} + H^+ \quad (1.3)$$

A detailed description of marine carbonate chemistry systematics and calculations can be found in Zeebe and Wolf-Gladrow (2001); here we will limit the discussion to a few basic details. The reactions between carbonate and hydrogen ions are governed by dissociation constants (K_1 and K_2), which depend on the thermodynamic seawater properties pressure (p), temperature (T) and salinity (S). The associated shift in carbonate ion speciation is shown in Figure 1.2, which displays the relative concentrations of $[CO_2]$, $[HCO_3^-]$ and $[CO_3^{2-}]$ versus seawater-pH at typical surface (T = 25 °C, S = 35, and p = 1 bar) and deep ocean conditions (T = 4 °C, S = 34.8, p = 401 bar). In contrast, the sum of all dissolved inorganic carbon (DIC) species and their alkalinity (i.e. the sum of their charges) are independent of T, S, and p when expressed in gravimetric units (i.e. $\mu mol\,kg^{-1}$, as opposed to the volumetric $\mu mol\,l^{-1}$). Because these six parameters are interrelated, the entire carbonate system can be determined if two of its components, in addition to temperature, salinity, and pressure, are known. Several programs facilitate computation of the carbonate system; see Further Reading for details.

One aspect that requires specific attention is the choice of pH scale. Four scales have been defined, the National Bureau of Standards (NBS), free hydrogen, seawater, and total scale; they differ in the chemical composition of their respective reference material and pH values determined for identical solutions differ by up to 0.15 units (Table 1.1). While this pH difference may appear small, it has significant consequences for carbon system calculations, as demonstrated in Table 1.1. For example, assuming the same T, S, p, pH, and DIC value to calculate pCO_2, but with pH defined on different scales, calculated pCO_2 differs by >150 µatm. Such large differences are inacceptable for carbon system determinations and must be avoided by all means. Fortuitously, pH scales are interrelated and values can be converted (see Zeebe and Wolf-Gladrow 2001), but this is only possible if studies cite the pH scale used.

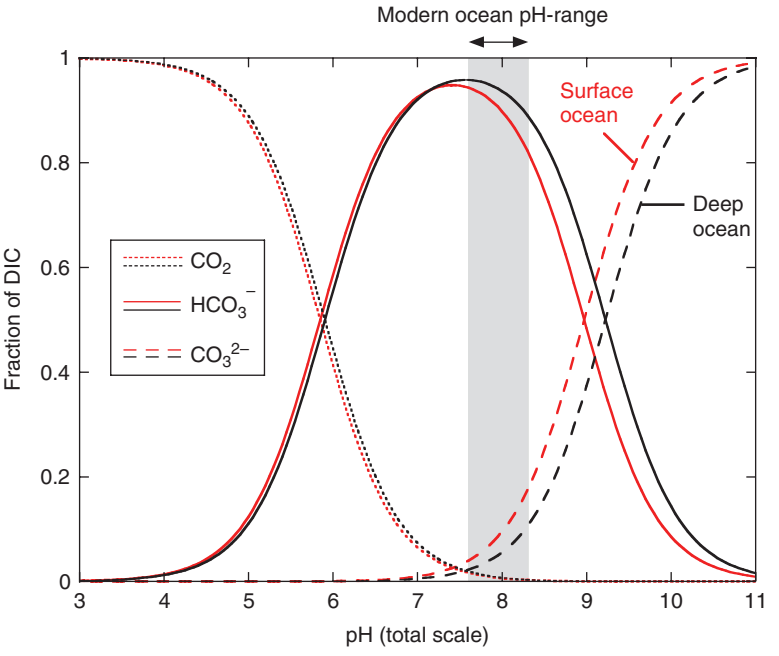

Figure 1.2 This Bjerrum plot displays relative concentrations of dissolved carbon species versus seawater-pH. Relative species concentrations were calculated using the CO2SYS program by Pierrot et al. (2006) with K_1 and K_2 according to Lueker et al. (2000), K_{SO4} according to Dickson (1990), total [B] after Lee et al. (2010), and using T = 25 °C, S = 35, p = 1 bar for the sea surface (red lines) and T = 4 °C, S = 34.8 p = 401 bar for the deep ocean (black lines). The modern range of seawater-pH is indicated by the gray bar.

Table 1.1 Definitions of pH scales, differences in scale-specific pH values in solutions of the same composition, and differences in pCO_2 calculated from solutions of similar composition but assuming pH = 8.10 for all four pH-scales.

Scale	Definition	pH value at TA = 2400 µmol kg^{-1}, DIC = 2100 µmol kg^{-1}, T = 25 °C, S = 35, p = 1 bar	pCO_2 at pH = 8.10, DIC = 2100 µmol kg^{-1}, T = 25 °C, S = 35, p = 1 bar
NBS (µmol kg^{-1} H_2O)	$pH_{NBS} = -\log a^{H+}$	8.162	513
Free (µmol kg^{-1} SW)	$pH_F = -\log [H+]_F$	8.133	477
Total (µmol kg^{-1} SW)	$pH_T = -\log ([H^+]_F + [HSO_4^-])$	8.025	363
Seawater (µmol kg^{-1} SW)	$pH_{SWS} = -\log ([H^+]_F + [HSO_4^-] + [HF])$	8.016	354

Calculations performed using the CO2SYS program (version 2.1) by Pierrot et al. (2006) with K_1 and K_2 according to Lueker et al. (2000), K_{SO4} according to Dickson (1990) and total [B] after Lee et al. (2010).

Because the boron equilibrium constants are reported for the total scale (Dickson 1990; Millero 1995), this book will present all data on the total scale.

Modern surface ocean pH is ~8.1 (total scale, TS), which is already ~0.1 pH units lower compared to the preindustrial, when atmospheric pCO_2 was ~120 ppm lower compared to today (Figure 1.1). Surface ocean pH continues to drop by ~0.002 units annually (Takahashi et al. 2014) and anthropogenic CO_2 slowly enters the intermediate and deep ocean via thermohaline circulation (Feely et al. 2004; Khatiwala et al. 2012; Sabine et al. 2004). Although the incremental accumulation of hydrogen ions resulting from dissolution of CO_2 will not actually turn seawater acidic (i.e. pH will not drop below 7), the trend towards decreasing pH has been termed *Ocean Acidification* (Caldeira and Wickett 2003). Depending on the source and extent of future anthropogenic carbon emissions, surface seawater pH is projected to decrease by an additional 0.1–0.7 pH units by the year 2200 (Figure 1.1). Laboratory experiments with various marine organisms and observations of naturally acidified ecosystems have highlighted the vulnerability of marine life to ocean acidification, but also the diversity of the biotic response (for a review see Doney et al. 2009).

Despite a wealth of experimental and observational work, projections of future ecosystem changes in the warming and acidifying ocean suffer from limited diversity and typically short duration of laboratory experiments, a shortcoming that can be compensated by the study of the geological record (e.g. Hönisch et al. 2012). Similarly, improving estimates of future warming requires better estimates of climate sensitivity, and the geological record offers a multitude of opportunities to study the interplay of CO_2 and temperature (Foster et al. 2017, PALEOSENS-project-members 2012). While polar ice provides the best archive for past CO_2 concentrations, continuous ice core records are currently limited to the past 800 000 years (Lüthi et al. 2008). Horizontal drilling into Antarctic blue ice has recovered isolated sections ~1 million years old (Higgins et al. 2015) and ~2.7 million years old (Yan et al. 2017), but the prospect of a continuous vertical record may not exceed 1.5 million years (Fischer et al. 2013). The study of geological archives therefore requires the use of proxies, i.e. measurable stand-ins for environmental parameters that can no longer be measured directly. CO_2- proxies have been developed for the terrestrial and the marine realm, and include the stomata density of fossil leaves, the carbon isotopic composition ($\delta^{13}C$) of marine biomarkers, and the boron isotopic composition and B/Ca ratios recorded in foraminifer shells, among others (e.g. Beerling and Royer 2011; Foster et al. 2017). Figures 1.3 and 1.4 display a selection of reconstructions over the past 800 000 and 65 million years, respectively. The functioning of the systematics, advantages, and shortcomings of the proxies displayed in these figures have been reviewed in Royer et al. (2001a) and Allen and Hönisch (2012). Because this book focuses on boron proxies, we will only mention the systematics of other proxies briefly.

Of the proxies shown, only the stomata (breathing cells) of vascular land plants are directly related to atmospheric pCO_2 – the stomatal index

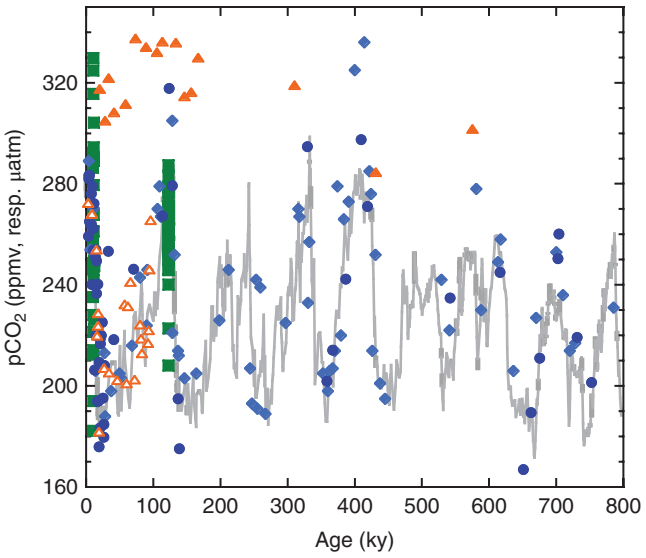

Figure 1.3 800 000 year record of atmospheric pCO_2 extracted from Antarctic ice cores (Lüthi et al. 2008; Petit et al. 1999; Siegenthaler et al. 2005) and reconstructed from planktic foraminiferal boron isotopes (dark blue circles, Henehan et al. 2013; Hönisch and Hemming 2005, Hönisch et al. 2009) and B/Ca ratios (light blue diamonds, Tripati et al. 2009; Yu et al. 2007), alkenones (orange triangles, Jasper and Hayes 1990; Zhang et al. 2013) and leaf stomata (green squares, Rundgren and Bennike 2002, Steinthorsdottir et al. 2013). Note that the calibration of Jasper and Hayes (1990) scaled the alkenone amplitude to the ice core pCO_2 amplitude. This is therefore not a completely independent reconstruction, but the shape of the proxy reconstruction matches the ice core data well. pCO_2 uncertainties are ~20 µatm for boron isotope estimates, ~30 µatm for B/Ca estimates, ~60 µatm for alkenone estimates and ~20 ppmv for leaf stomata estimates.

decreases as atmospheric pCO_2 increases, such that water loss via evaporation can be minimized when CO_2 is abundant (e.g. Royer et al. 2001b), but see also Franks et al. (2014) for additional environmental and stomatal anatomy controls on leaf gas exchange. Alkenone pCO_2 estimates are based on the carbon isotope fractionation that occurs during photosynthesis performed by marine haptophytes, where $\delta^{13}C_{alkenone}$ is inversely related to aqueous $[CO_2]$, but also depends on algal growth rate (i.e. nutrient supply) and cell geometry (e.g. Henderiks and Pagani 2007). As such, alkenone reconstructions require a few auxiliary data, including estimates of $\delta^{13}C$ of DIC, temperature, nutrients, and cell geometry (e.g. Zhang et al. 2013), all of which can be estimated from respective marine proxy records. Boron isotopes and B/Ca ratios in planktic foraminifer shells are not directly related to pCO_2 but rather to seawater acidity, and thus require a second parameter of the carbonate system to estimate pCO_2 via pH. The second parameter is often given by an assumption of total alkalinity, which changes little on Pleistocene time scales, but is more uncertain on multi-million year time scales (Caves et al. 2016; Ridgwell 2005; Tyrrell and Zeebe 2004). Boron proxy-to-pCO_2 translations also require estimates of temperature and salinity, in addition to knowledge of the boron isotopic composition ($\delta^{11}B_{sw}$),

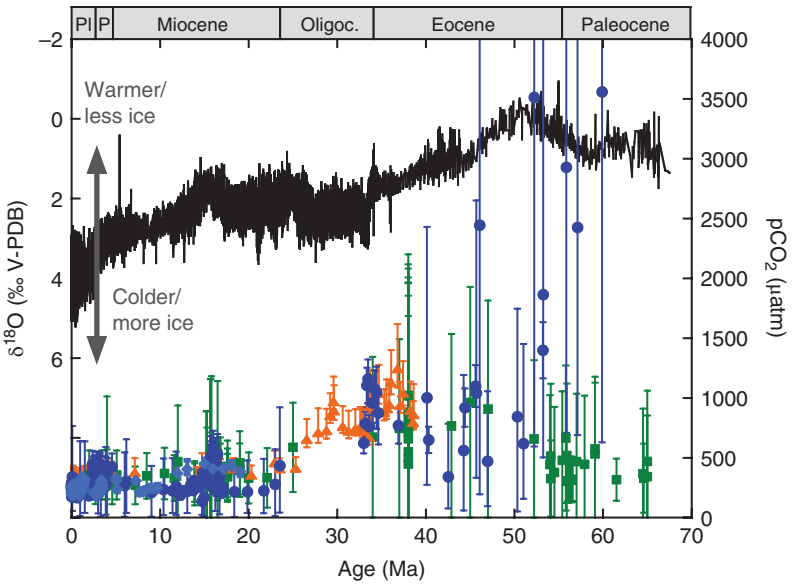

Figure 1.4 Proxy estimates of Cenozoic climate change (as inferred from benthic foraminiferal $\delta^{18}O$, Zachos et al. 2008) and atmospheric pCO_2 reconstructed from planktic foraminiferal boron isotopes (dark blue circles, Anagnostou et al. 2016; Badger et al. 2013; Bartoli et al. 2011; Foster et al. 2012; Greenop et al. 2014; Hönisch et al. 2009; Martínez-Botí et al. 2015; Pearson et al. 2009; Seki et al. 2010) and B/Ca ratios (light blue diamonds, Tripati et al. 2009), alkenones (orange triangles, Zhang et al. 2013) and leaf stomata (green squares, van der Burgh et al. 1993; Kürschner et al. 1996, 2001; McElwain 1998; Royer et al. 2001a; Beerling et al. 2002; Greenwood et al. 2003; Royer 2003; Kürschner et al. 2008; Retallack 2009; Smith et al. 2010; Doria et al. 2011). Geological epochs are indicated by the gray bar. Whereas Pleistocene (Pl) and Pliocene (P) pCO_2 estimates compare fairly well, Miocene records diverge by ~150 µatm and Paleocene/Eocene records by ~2000 µatm. Similarly, pCO_2 uncertainties vary by proxy and increase further back in time. Such large uncertainties compromise estimates of past climate sensitivity.

boron and calcium concentrations of seawater. The details of these parameters and translations will be explained later in this book, for now it suffices to say that pCO_2 reconstructions from proxies are more complicated than the extraction of actual CO_2 from air trapped in polar ice. However, despite the complexity of the respective translation process, validation of proxy estimates relative to ice core pCO_2 (Figure 1.3) shows convincing results. Going further back in time, pCO_2 estimates from different proxies show relatively consistent values until ~40 Ma, but diverge greatly during the early Eocene and Paleocene, with $\delta^{11}B$ estimates showing the highest pCO_2 values (Figure 1.4).

While these proxy estimates have greatly enhanced our understanding of Earth's climate system, the uncertainties associated with all of these pCO_2 estimates preclude accurate estimates of climate sensitivity (PALEOSENS-project-members 2012). Improvements have been made over the past few years but are still needed for all proxies. In particular, some of the boron proxy records shown in Figures 1.3 and 1.4 are no longer considered scientifically

sound, and we will discuss individual boron proxy records in detail. However, this book will not only focus on atmospheric pCO_2. Estimates of seawater pH in coral reefs and carbon storage in the deep ocean are all aspects that contribute to our understanding of the marine carbon system, climate, and ecosystem dynamics. These properties can be reconstructed with boron proxy estimates in marine carbonates as different as shallow and deep-water coral skeletons, planktic, and benthic foraminifer shells, brachiopod shells, and inorganic precipitates. In addition to pCO_2 estimates beyond ice cores, boron proxies thereby provide a plethora of opportunities to decipher the causes of past carbon cycle variations and their effect on marine ecosystems.

Acknowledgments

We acknowledge the World Climate Research Programme's Working Group on Coupled Modeling, which is responsible for CMIP, and we thank the climate modeling groups (listed at http://cmip-pcmdi.llnl.gov/cmip5/docs/CMIP5_modeling_groups.pdf) for producing and making available their model output. For CMIP, the U.S. Department of Energy's Program for Climate Model Diagnosis and Intercomparison provides coordinating support and led development of software infrastructure in partnership with the Global Organization for Earth System Science Portals.

References

Allen, K.A. and Hönisch, B. (2012). The planktic foraminiferal B/Ca proxy for seawater carbonate chemistry: a critical evaluation. *Earth and Planetary Science Letters* 345–348: 203–211.

Anagnostou, E., John, E.H., Edgar, K.M. et al. (2016). Changing atmospheric CO_2 concentration was the primary driver of early Cenozoic climate. *Nature* 533 (7603): 380–384.

Arrhenius, S. (1896). On the influence of carbonic acid in the air upon the temperature on the ground. *Philosophical Magazine* 41: 237–276.

Badger, M.P.S., Lear, C.H., Pancost, R.D. et al. (2013). CO_2 drawdown following the middle Miocene expansion of the Antarctic Ice Sheet. *Paleoceanography* 28 (1): 42–53.

Barnola, J.M., Raynaud, D., Korotkevich, Y.S., and Lorius, C. (1987). Vostok ice core provides 160,000-year record of atmospheric CO_2. *Nature* 329 (6138): 408–414.

Bartoli, G., Hönisch, B., and Zeebe, R.E. (2011). Atmospheric CO_2 decline during the Pliocene intensification of Northern Hemisphere glaciations. *Paleoceanography* 26 (4): PA4213.

Beerling, D.J. and Royer, D.L. (2011). Convergent Cenozoic CO_2 history. *Nature Geoscience* 4 (7): 418–420.

Beerling, D.J., Lomax, B.H., Royer, D.L. et al. (2002). An atmospheric pCO_2 reconstruction across the cretaceous-tertiary boundary from leaf megafossils. *Proceedings of the National Academy of Sciences of the United States of America* 99 (12): 7836–7840.

van der Burgh, J., Visscher, H., Dilcher, D.L., and Kürschner, W.M. (1993). Paleoatmospheric signatures in Neogene fossil leaves. *Science* 260: 1788–1790.

Caldeira, K. and Wicket, M.E. (2003). Anthropogenic carbon and ocean pH. *Nature* 425: 365.

Caves, J.K., Jost, A.B., Lau, K.V., and Maher, K. (2016). Cenozoic carbon cycle imbalances and a variable weathering feedback. *Earth and Planetary Science Letters* 450: 152–163.

Dickson, A.G. (1990). Standard potential of the reaction: $AgCl(s)+1/2H_2(g)=Ag(s)+HCl(aq)$, and the standard acidity constant of the ion HSO_4^- in synthetic seawater from 273.15 to 318.15K. *The Journal of Chemical Thermodynamics* 22: 113–127.

Dlugokencky, E. and Tans, P. (2017) *Mauna Loa CO2 annual mean data*, NOAA/ESRL (www.esrl.noaa.gov/gmd/ccgg/trends/)

Doney, S.C., Fabry, V.J., Feely, R.A., and Kleypas, J.A. (2009). Ocean acidification: the other CO_2 problem. *Annual Review of Marine Science* 1: 169–192.

Doria, G., Royer, D.L., Wolfe, A.P. et al. (2011). Declining atmospheric CO_2 during the late middle Eocene climate transition. *American Journal of Science* 311: 63–75.

Feely, R.A., Sabine, C.L., Lee, K. et al. (2004). Impact of anthropogenic CO_2 on the $CaCO_3$ system in the oceans. *Science* 305: 362–366.

Fischer, H., Severinghaus, J., Brook, E. et al. (2013). Where to find 1.5 million yr old ice for the IPICS "oldest-ice" ice core. *Climate of the Past* 9 (6): 2489–2505.

Foster, G.L., Lear, C.H., and Rae, J.W.B. (2012). The evolution of pCO_2, ice volume and climate during the middle Miocene. *Earth and Planetary Science Letters* 341–344: 243–254.

Foster, G.L., Royer, D.L., and Lunt, D.J. (2017). Future climate forcing potentially without precedent in the last 420 million years. *Nature Communications* 8: 14845.

Franks, P.J., Royer, D.L., Beerling, D.J. et al. (2014). New constraints on atmospheric CO_2 concentration for the Phanerozoic. *Geophysical Research Letters* 41: 4685–4694.

Gattuso, J.-P., Epitalon, J.-M., Lavigne, H. et al. (2017) seacarb: Seawater Carbonate Chemistry, CRAN-R.project.org, https://cran.r-project.org/package=seacarb.

Greenop, R., Foster, G.L., Wilson, P.A., and Lear, C.H. (2014). Middle Miocene climate instability associated with high-amplitude CO_2 variability. *Paleoceanography* 29 (9): 845–853.

Greenwood, D.R., Scarr, M.J., and Christophel, D.C. (2003). Leaf stomatal frequency in the Australian tropical rainforest tree *Neolitsea dealbata* (Lauraceae) as a proxy measure of atmospheric pCO_2. *Palaeogeography, Palaeoclimatology, Palaeoecology* 196: 375–393.

Henderiks, J. and Pagani, M. (2007). Refining ancient carbon dioxide estimates: significance of coccolithophore cell size for alkenone-based pCO_2 records. *Paleoceanography* 22.

Henehan, M.J., Rae, J.W.B., Foster, G.L. et al. (2013). Calibration of the boron isotope proxy in the planktonic foraminifera *Globigerinoides ruber* for use in palaeo-CO_2 reconstruction. *Earth and Planetary Science Letters* 364: 111–122.

van Heuven, S., Pierrot, D., Lewis, E., and Wallace, D.W.R. (2009) MATLAB Program Developed for CO_2 System Calculations, ORNL/CDIAC-105b.

Higgins, J.A., Kurbatov, A.V., Spaulding, N.E. et al. (2015). Atmospheric composition 1 million years ago from blue ice in the Allan Hills, Antarctica. *Proceedings of the National Academy of Sciences* 112 (22): 6887–6891.

Hönisch, B. and Hemming, N.G. (2005). Surface ocean pH response to variations in pCO_2 through two full glacial cycles. *Earth and Planetary Science Letters* 236 (1–2): 305–314.

Hönisch, B., Hemming, N.G., Archer, D. et al. (2009). Atmospheric carbon dioxide concentration across the mid-Pleistocene transition. *Science* 324 (5934): 1551–1554.

Hönisch, B., Ridgwell, A., Schmidt, D.N. et al. (2012). The geological record of ocean acidification. *Science* 335 (6072): 1058–1063.

IPCC (2013) Climate Change 2013: The Physical Science Basis. Contribution of Working Group I to the Fifth Assessment Report of the Intergovernmental Panel on Climate Change Cambridge University Press, Cambridge. http://www.ipcc.ch/report/ar5/

Jasper, J.P. and Hayes, J.M. (1990). A carbon isotope record of CO_2 levels during the late quaternary. *Nature* 347 (6292): 462–464.

Jouzel, J., Lorius, C., Petit, J.R. et al. (1987). Vostok ice core: a continuous isotope temperature record over the last climatic cycle (160,000 years). *Nature* 329 (6138): 403–408.

Keeling, C.D., Bacastow, R.B., Bainbridge, A.E. et al. (1976). Atmospheric carbon dioxide variations at Mauna Loa Observatory, Hawaii. *Tellus* 28: 538–551.

Khatiwala, S., Primeau, F., and Holzer, M. (2012). Ventilation of the deep ocean constrained with tracer observations and implications for radiocarbon estimates of ideal mean age. *Earth and Planetary Science Letters* 325–326: 116–125.

Kürschner, W.M., Kvacek, Z., and Dilcher, D.L. (2008). The impact of Miocene atmospheric carbon dioxide fluctuations on climate and the evolution of terrestrial ecosystems. *Proceedings of the National Academy of Sciences of the United States of America* 105: 449–453.

Kürschner, W.M., van der Burgh, J., Visscher, H., and Dilcher, D.L. (1996). Oak leaves as biosensors of late Neogene and early Pleistocene paleoatmospheric CO_2 concentrations. *Marine Micropaleontology* 27: 299–312.

Kürschner, W.M., Wagner, F., Dilcher, D.L., and Visscher, H. (2001). Using fossil leaves for the reconstruction of Cenozoic paleoatmospheric CO_2 concentrations. In: *Geological Perspectives of Global Climate Change* (ed. L.C. Gerhard, W.E. Harrison and B.M. Hanson), 169–189. Tulsa: The American Association of Petroleum Geologists.

Lee, K., Kim, T.-W., Byrne, R.H. et al. (2010). The universal ratio of boron to chlorinity for the North Pacific and North Atlantic oceans. *Geochimica et Cosmochimica Acta* 74 (6): 1801–1811.

Lueker, T.J., Dickson, A.G., and Keeling, C.D. (2000). Ocean pCO_2 calculated from dissolved inorganic carbon, alkalinity, and equations for K1 and K2: validation based on laboratory measurements of CO_2 in gas and seawater at equilibrium. *Marine Chemistry* 70 (1–3): 105–119.

Lüthi, D., Le Floch, M., Bereiter, B. et al. (2008). High-resolution carbon dioxide concentration record 650,000–800,000 years before present. *Nature* 453 (7193): 379–382.

Martínez-Botí, M.A., Foster, G.L., Chalk, T.B. et al. (2015). Plio-Pleistocene climate sensitivity evaluated using high-resolution CO_2 records. *Nature* 518 (7537): 49–54.

McElwain, J.C. (1998). Do fossil plants signal palaeoatmospheric CO_2 concentration in the geological past? *Philosophical Transactions of the Royal Society London B* 353: 83–96.

Meinshausen, M., Smith, S.J., Calvin, K. et al. (2011). The RCP greenhouse gas concentrations and their extensions from 1765 to 2300. *Climatic Change* 109 (1–2): 213–241.

Millero, F.J. (1995). Thermodynamics of the carbon dioxide system in the oceans. *Geochimica et Cosmochimica Acta* 59 (4): 661–667.

Moss, R.H., Edmonds, J.A., Hibbard, K.A. et al. (2010). The next generation of scenarios for climate change research and assessment. *Nature* 463 (7282): 747–756.

PALEOSENS-project-members (2012). Making sense of paleoclimate sensitivity. *Nature* 419: 683–691.

Pearson, P.N., Foster, G.L., and Wade, B.S. (2009). Atmospheric carbon dioxide through the Eocene-Oligocene climate transition. *Nature* 461 (7267): 1110–U204.

Petit, J.R., Jouzel, J., Raynaud, D. et al. (1999). Climate and atmospheric history of the past 420,000 years from the Vostok ice core, Antarctica. *Nature* 399: 429–436.

Pierrot, D., Lewis, E., and Wallace, D.W.R. (2006) MS Excel Program Developed for CO_2 System Calculations, ORNL/CDIAC-105a.

Raynaud, D. and Barnola, J.M. (1985). An Antarctic ice core reveals atmospheric CO_2 variations over the past few centuries. *Nature* 315 (6017): 309–311.

Retallack, G.J. (2009). Greenhouse crises of the past 300 million years. *Geological Society of America Bulletin* 121: 1441–1455.

Ridgwell, A. (2005). A mid Mesozoic revolution in the regulation of ocean chemistry. *Marine Geology* 217 (3–4): 339–357.

Royer, D.L. (2003). Estimating latest cretaceous and tertiary atmospheric CO_2 concentration from stomatal indices. In: *Causes and Consequences of Globally Warm Climates in the Early Paleogene*, Geological Society of America Special Paper 369 (ed. S.L. Wing, P.D. Gingerich, B. Schmitz and E. Thomas), 79–93. Boulder: Geological Society of America.

Royer, D.L., Berner, R.A., and Beerling, D.J. (2001a). Phanerozoic atmospheric CO_2 change: evaluating geochemical and paleobiological approaches. *Earth-Science Reviews* 54: 349–392.

Royer, D.L., Wing, S.L., Beerling, D.J. et al. (2001b). Paleobotanical evidence for near present-day levels of atmospheric CO_2 during part of the tertiary. *Science* 292 (5525): 2310–2313.

Rundgren, M. and Bennike, O. (2002). Century-scale changes of atmospheric CO_2 during the last interglacial. *Geology* 30 (2): 187–189.

Sabine, C.L., Feely, R.A., Gruber, N. et al. (2004). The oceanic sink for anthropogenic CO_2. *Science* 305: 367–371.

Seki, O., Foster, G.L., Schmidt, D.N. et al. (2010). Alkenone and boron-based Pliocene pCO_2 records. *Earth and Planetary Science Letters* 292 (1–2): 201–211.

Siegenthaler, U., Stocker, T.F., Monnin, E. et al. (2005). Stable carbon cycle-climate relationship during the Late Pleistocene. *Science* 310 (5752): 1313–1317.

Smith, R.Y., Greenwood, D.R., and Basinger, J.F. (2010). Estimating paleoatmospheric pCO_2 during the early Eocene climatic optimum from stomatal frequency of *Ginkgo*, Okanagan Highlands, British Columbia, Canada. *Palaeogeography, Palaeoclimatology, Palaeoecology* 293: 120–131.

Steinthorsdottir, M., Wohlfarth, B., Kylander, M.E. et al. (2013). Stomatal proxy record of CO2 concentrations from the last termination suggests an important role for CO2 at climate change transitions. *Quaternary Science Reviews* 68: 43–58.

Takahashi, T., Sutherland, S.C., Chipman, D.W. et al. (2014). Climatological distributions of pH, pCO_2, total CO_2, alkalinity, and $CaCO_3$ saturation in the global surface ocean, and temporal changes at selected locations. *Marine Chemistry* 164: 95–125.

Taylor, K.E., Stouffer, R.J., and Meehl, G.A. (2011). An overview of CMIP5 and the experiment design. *Bulletin of the American Meteorological Society* 93 (4): 485–498.

Tripati, A.K., Roberts, C.D., and Eagle, R.A. (2009). Coupling of CO_2 and ice sheet stability over major climate transitions of the last 20 million years. *Science* doi: 10.1126/science.1178296.

Tyrrell, T. and Zeebe, R.E. (2004). History of carbonate ion concentration over the last 100 million years. *Geochimica et Cosmochimica Acta* 68 (17): 3521–3530.

Yan, Y., J. Ng, J. Higgins et al. (2017) 2.7-Million-Year-Old Ice from Allan Hills Blue Ice Areas, East Antarctica Reveals Climate Snapshots Since Early Pleistocene, Goldschmidt Conference, Paris.

Yu, J., Elderfield, H., and Hönisch, B. (2007). B/Ca in planktonic foraminifera as a proxy for surface seawater pH. *Paleoceanography* 22: doi: 10.1029/2006PA001347.

Zachos, J.C., Dickens, G.R., and Zeebe, R.E. (2008). An early Cenozoic perspective on greenhouse warming and carbon-cycle dynamics. *Nature* 451 (7176): 279–283.

Zeebe, R.E. and Wolf-Gladrow, D.A. (2001). *CO_2 in seawater: Equilibrium, kinetics, isotopes*, vol. 65, 346. Elsevier.

Zhang, Y.G., Pagani, M., Liu, Z. et al. (2013). A 40-million-year history of atmospheric CO_2. *Philosophical Transactions of the Royal Society A: Mathematical, Physical and Engineering Sciences* 371 (2001).

Further Reading/Resources

CO_2 in seawater: Equilibrium, Kinetics, Isotopes, by Zeebe and Wolf-Gladrow, Elsevier Oceanography Series, Volume 65, 360 pp., eBook ISBN: **9780080529226, 2001** – the resource for all questions on ocean carbonate chemistry

Ocean carbonate chemistry calculation programs can be found at:

CO2SYS for EXCEL (Pierrot et al. 2006) and Matlab (van Heuven et al. 2009): http://cdiac.ornl.gov/oceans/co2rprt.html

csys.m, a Matlab program that accompanies ***CO_2 in seawater*** by Zeebe and Wolf-Gladrow (2001): http://www.soest.hawaii.edu/oceanography/faculty/zeebe_files/CO_2_System_in_Seawater/csys.html

seacarb (Gattuso et al. 2017): https://CRAN.R-project.org/package=seacarb